162. Mechanistic Details of the Fe^+-Mediated C–C and C–H Bond Activations in Propane: A Theoretical Investigation

by **Max C. Holthausen**[1]) and **Wolfram Koch***

Institut für Organische Chemie der Technischen Universität Berlin, Strasse des 17. Juni 135, D-10623 Berlin

(13.V.96)

Quantum-chemical calculations employing a density-functional theory/*Hartree-Fock* hybrid method (B3LYP) have been used to explore the mechanistic details of the C–C and C–H bond-activation processes in propane mediated by a bare Fe^+ ion. While the theoretically predicted results are in complete accord with all available experimental data, they give rise to a different mechanistic picture than envisaged previously. In contrast to earlier speculations, the activation barriers for the initial insertion steps of Fe^+ into a C–H or C–C bond are found to be significantly below the $Fe^+ + C_3H_8$ channel. The rate-determining steps for both, the C–C and the C–H bond activation branches of the $[FeC_3H_8]^+$ potential-energy surface rather occur late on the respective reaction coordinates and are connected with saddle points of concerted rearrangement processes. The C–C bond activation, which leads to the exothermic reductive elimination of methane, occurs *via* the C–C inserted species and not as a side channel originating from a C–H inserted ion, as assumed hitherto. For the C–H bond-activation processes, which finally results in the exothermic expulsion of molecular hydrogen, two energetically similar reaction channels for an [1,2]-elimination exist. The results clearly show, that an [1,3]-H_2-elimination mechanism cannot compete with the [1,2]-elimination paths, in line with the experimental findings. Overall, a lower energy demand for the reductive elimination of methane compared to the loss of H_2 is obtained, straightforwardly explaining the preference of the former process observed experimentally.

Introduction. – The C–H and C–C bond activations of alkanes brought about by bare transition-metal ions are of paramount interest in various areas of chemical research, such as organic chemistry, biochemistry, and, probably most importantly [1], catalytic research. The oxidative addition and reductive elimination of ligands are two of the most fundamental steps in reactions occurring at metal centers in catalytic processes. A rigorous understanding of these elementary processes taking place at reactive centers is a prerequisite for the development of guidelines for rationalizing and predicting the corresponding chemical transformations. From an experimental point of view, mass spectrometric studies of gas-phase reactions between transition-metal ions and organic substrates are a powerful tool to assess intrinsic binding properties and the reactivity of these species without the cooperative influences of further ligands, counter-ions, or solvent molecules (for recent reviews, see [2]). Such techniques have provided a wealth of accurate thermochemical data, such as M^+–R binding energies, for a wide variety of organometallic species. In spite of this impressive progress, a complete characterization of the actual reaction mechanisms, *i.e.*, explicit information on the structural and energetical details of all intermediates and transition structures involved in the course of a particular reaction, is, however, possible only in a limited number of cases by experimen-

[1]) Present address: *Cherry L. Emerson* Center for Scientific Computation and Department of Chemistry, Emory University, Atlanta, Georgia 30322, USA.

tal means alone. Quantum-chemical calculations offer in principle a complementary source of information. However, even if only qualitative accuracy in the field of open-shell transition-metal species is desired in the framework of conventional *ab initio* molecular-orbital theory, a sophisticated treatment of both near degeneracy as well as dynamic electron correlation effects in combination with large and flexible one-particle basis sets is required, and the application of such methods is usually restricted to rather small molecules (see, *e.g.* [3]). As a promising alternative, which combines reasonable accuracy with computational efficiency, density-functional theory (DFT), and in particular DFT/*Hartree-Fock* hybrid methods have recently attracted considerable attention. These methods have been successfully applied by us and others to study various open-shell transition-metal species (see, *e.g.* [4]). In recent investigations, we employed the DFT/HF approach to elucidate complete reaction sequences involving open-shell transition-metal species: the reactions of Fe^+ and of Co^+ with ethane, which represent prototype systems for transition-metal-cation-mediated C–H and C–C bond activations in alkanes [5]. However, in gas-phase experiments, propane is the smallest alkane for which the Fe^+-mediated reductive elimination of CH_4 and H_2 can be observed at thermal energies. An interesting question is why propane is reactive and ethane is not, even though the loss of H_2 is in both cases exothermic. Assuming the same fundamental reaction mechanisms for both alkanes, a reasonable explanation for the increased reactivity with alkane size is the increasing polarizability of the neutral molecule[2]). However, in the propane system, two types of C–H bonds (primary and secondary) are present, and a much more complex chemistry is possible as compared to the ethane analogue. For the reaction of the latter, our earlier studies provided a detailed and consistent view on the mechanisms of C–H and C–C activation processes mediated by a Fe^+ cation. Both reaction sequences consist of two elementary steps each: of these, the initial steps – insertion of Fe^+ into the C–C or C–H bond – are energetically less demanding than the subsequent ones. We unambiguously identified concerted elementary steps, which directly connect the C–C- or C–H-inserted precursor ions with the product complexes of CH_4 or H_2, respectively, as rate-limiting for the expulsion of H_2 and CH_4 [5]. It is of particular interest, whether this mechanistic scenario established for the ethane activation will carry over to the propane system, or whether different reaction mechanisms are preferred. In the present contribution, we provide a comprehensive quantum-chemical picture of the reactions of cationic iron with the next higher alkane, *i.e.*, propane. This paper is organized as follows: after a brief introduction into the applied DFT/HF approach, we give the results of calibration calculations in order to establish the accuracy that can be expected from this computational scheme. We then present an overview of the experimental information available in the literature, and how these are interpreted in terms of mechanistic details of the bond-activation processes. Next, the theoretically predicted pathways of the C–C and C–H bond activations, in which all minima and saddle points on the $[FeC_3H_8]^+$ potential energy surface (PES) relevant for these reactions are characterized, are presented in detail, and the results and its implications are analyzed in light of the previous experimental findings. Finally, the conclusions from this investigation are summarized.

---

[2]) This is, the higher polarizability causes a larger attractive electrostatic interaction, which, in the case of Fe^+ + propane, is large enough to overcome the reaction barriers.

Computational Details. – The computational approach employed in the present study closely follows our earlier work and has been described in detail in these publications [4a,b] [5]. We use the 'Becke-3-LYP' functional [6] (abbreviated as B3LYP) as implemented in the DFT module of Gaussian92/DFT [7]. This functional is combined with the standard-D95**-polarized double-zeta basis set [8] for C and H. For Fe, the (14s 9p 5d) primitive set of *Wachters* [9] supplemented with one diffuse p-function ($\alpha = 0.1150$) and one diffuse d-function according to *Hay* [10] is utilized, resulting in a (62111111|33121|411) → (8s 5p 3d) contraction [9]. All computations have been performed employing the 'finegrid' option for the atomic integration grids. Stationary points were localized using analytical gradients, and their characters (minimum, transition structure, or higher-order saddle point) were determined from the analytically computed force-constant matrices. All structures discussed in the text correspond to fully optimized geometries with both, the gradients as well as the displacements from analytical second derivatives below the standard convergence criteria. To allow for a more direct comparison to experiment, we corrected our calculated energies to ΔU at 0 K (equivalent to ΔH or ΔG at this temperature) by including zero-point vibrational energy (*ZPVE*) contributions. Due to known problems [11] of rotational invariance in the numerical integration techniques in Gaussian92/DFT, the frequency calculations of some structures showed non-zero rotational frequencies. Since deviations in the lowest frequencies contribute directly to the calculation of thermodynamic properties, we do not correct our results for thermal contributions, which are expected to be very small anyway.

Calibration. – We commence this investigation with a comparison of theoretically predicted binding energies of a representative set of species relevant for the $Fe^+ + C_3H_8$ interaction to the experimentally determined ones, as summarized in *Table 1*. For the hydrocarbons, C–H bond dissociation energies (*BDE*) are excellently reproduced at the B3LYP level of theory, while C–C binding energies are – in contrast to what one should expect from a DFT-based method – underestimated by some 8 kcal mol^{-1}[3]). The Fe–C and Fe–H binding energies are without exception overestimated by the B3LYP approach, the mean error amounts to 11.1 kcal mol^{-1}. However, the degree of overbinding varies significantly: the deviation is largest for the weakly, mostly electrostatically bound species such as $Fe(C_2H_4)^+$, $Fe(C_3H_8)^+$, and $Fe(C_3H_6)^+$, where the experimental binding energies[4]) are overestimated significantly by 17, 18, and 19 kcal mol^{-1} by the B3LYP calculations. The agreement is much better for the covalently bound ions $FeCH_2^+$, FeH^+, $FeCH_3^+$, and $FeC_2H_5^+$, where the overbinding does not exceed 9 kcal mol^{-1}. Part of this overestimation of binding energies can certainly be traced back to the well-known overbinding tendency inherent to any density-functional method. Further, deficiencies in the one-particle description of the *Kohn-Sham* orbitals cannot be ruled out as contributing to the overall error, even though we do not expect this to be significant. A third and very important reason can be found in the fact that the B3LYP scheme erroneously predicts the electronic ground state of Fe^+ as ^4F ($3d^7$) separated from the ^6D ($3d^6\,4s^1$) state by 3.2 kcal mol^{-1}. Experimentally, the ground state is ^6D with an j-averaged excitation

---

[3]) This is rather an effect of the employed functional than a basis-set effect: employing the larger 6-311 + G(3df,2p) basis set, the *BDE*(C–C) in ethane is 82 kcal mol^{-1} (D95**: 83 kcal mol^{-1}).

[4]) All experimental Fe^+–L bond-dissociation energies are taken from the very recent compilation [12].

energy to the ^4F state of 5.8 kcal mol^{-1} [13]. Again, this error of 9 kcal mol^{-1} reflects a well-known problem in DFT, *i.e.*, the bias towards d^n over $d^{n-1}s^1$ configurations (see, *e.g.* [14]). We did not simply correct the Fe^+ ground-state asymptote for the experimental splitting, which would reduce the mean error in *Table 1* significantly and is most plausible for the mainly electrostatic character of the binding in the quartet-spin-state complexes $Fe(H_2)^+$, $Fe(CH_4)^+$, $Fe(C_2H_6)^+$, $Fe(C_2H_4)^+$, $Fe(C_3H_8)^+$, and $Fe(C_3H_6)^+$. Such a correction does not account for the individual accuracy in the description of different bonding situations. We would assume that the underlying reason for the error in the atomic regime is also present in the description of the molecular complexes with their different amount of d^n and $d^{n-1}s^1$ character of the iron cation. At a first glance, a promising approach here would be a case-dependent correction according to the occupation numbers of d-orbitals, following ideas recently advocated also for DFT calculations by *Ricca* and *Bauschlicher* [4d]. However, it has recently been shown [15] that, in modern gradient-corrected functionals, errors are not uniformly distributed over a molecular environment, and that error compensation effects could be in part responsible for the good performance of gradient-corrected DFT computations. No such careful analysis is existent for the presently used HF/DFT hybrid functionals, and we feel that more experience has to be collected on the performance of these methods before a plausible correction scheme becomes obvious.

Table 1. *Experimental and Calculated Binding Energies* [kcal mol^{-1}]

Species	Exper.[a])	Calc.	Species	Exper.[b])	Calc.
$Fe{=}CH_2^+$ ($^4B_1$)	81.5 ± 0.9	83	H–H	104	107
Fe^+–H ($^5\Delta$)	48.9 ± 1.4	58	CH_3–H	105	103
Fe^+–CH_3 (^5E)	54.6 ± 1.1	62	C_2H_5–H	100	100
Fe^+–C_2H_5 ($^5A''$)	55.7 ± 2.1	63	C_3H_7–H	98	95
$Fe(CH_4)^+$ (^4E)	13.7 ± 0.8	24	CH_3–CH_3	90	83
$Fe(C_2H_6)^+$ ($^4A''$)	15.2 ± 1.4	27	C_2H_5–CH_3	88	80
$Fe(C_3H_8)^+$ ($^4B_2$)	17.9 ± 1.0	36	$CH_2{=}CH_2$	174	165
$Fe(H_2)^+$ ($^4B_2$)	5.2 ± 1.3	17			
$Fe(C_2H_4)^+$ ($^4B_2$)	34.7 ± 1.4	52			
$Fe(C_3H_6)^+$ (^4A)	34.7 ± 1.7[c])	53			

[a]) Experimental data taken from [12]. [b]) Experimental data taken from [16]. [c]) A value of 37.0 ± 0.3 kcal mol^{-1} has been determined for the binding energy of $Fe(C_3H_6)^+$ [17].

From this part of our calibration, we can conclude that, whenever we are dealing with dissociation processes involving the atomic Fe^+ ion, binding energies will be significantly exaggerated. However, our goal in the present work is to describe the interesting properties of the $[FeC_3H_8]^+$ potential-energy surface (PES) rather than to give quantitative predictions of binding energies. To this end, the ability to correctly reproduce the relative energies of various parts of this PES is of much greater importance than to have absolute binding energies. Here, *Table 2* shows the relative stabilities of the various fragmentation products relative to the energetically least favorable asymptote, *i.e.*, FeH^+ ($^5\Delta$) + $\dot{C}_3H_7$, arbitrarily chosen as zero. The experimental and computed data agree very well, the only exception being the one where a bare iron cation is involved (Fe^+ (^6D) + C_2H_6). This asymptote is computed as too high by 13 kcal mol^{-1}, completely in line with the reasoning

discussed above. If this particularly problematic dissociation is excluded, the unsigned mean error amounts to merely 3.2 kcal mol^{-1}. Thus, we are confident that the relative energetics of the PES of $[FeC_3H_8]^+$ is described reliably at the B3LYP level, even though the aforementioned shortcomings of the chosen B3LYP approach to some extent limit the predictive power in quantitative terms.

Table 2. *Experimental and Calculated Relative Energies of the Exit Channels Relative to Separated* $FeH^+ (^5\Delta) + \dot{C}_3H_7$ [kcal mol^{-1}]

Exit channel	Exper.[a])	Calc.
$Fe^+ (^6D) + C_3H_8$	−50	−37
$Fe(C_3H_6)^+ + H_2$	−57	−61
$Fe(C_2H_4)^+ + CH_4$	−67	−65
$FeCH_2^+ + C_2H_6$	−34	−29
$FeCH_3 + \dot{C}_2H_5$	−18	−20
$FeC_2H_5^+ + \dot{C}H_3$	−18	−21
$FeH^+ + \dot{C}_3H_7$	0	0

[a]) Experimental data taken from [16].

Experimental Background. – The gas-phase reactions of bare transition-metal ions with small alkanes have been studied intensively by mass spectrometry employing various techniques [2]. The reactions involving propane are of considerable interest, since, unlike for the smaller alkane ethane, exothermic processes are observed at thermal energies which lead to reductive eliminations of CH_4 and H_2. Under these conditions, both processes occur rather inefficient, however. This indicates the existences of significant reaction barriers near the energy of the entrance channel. At elevated kinetic energies, additional fragmentations indicative of direct C–H and C–C bond cleavages occur. In particular, the interaction of Fe^+ with propane has been intensively studied by various groups [18]. At thermal energies, *i.e.*, without deposition of additional kinetic energy in the reaction system, exothermic reactions leading to Fe^+-alkene complexes according to $Fe^+ + C_3H_8 \rightarrow Fe(C_3H_6)^+ + H_2$ and $Fe^+ + C_3H_8 \rightarrow Fe(C_2H_4)^+ + CH_4$ are observed with a 3:1 preference of the CH_4 extrusion over H_2 elimination. The most relevant experimental study of the PES of $[FeC_3H_8]^+$ in the context of our calculations is the recent mass-spectrometrical account by *van Koppen et al.* [19]. These authors extensively studied the PES of $[FeC_3H_8]^+$ and employed elaborate isotopic labeling experiments and kinetic-energy release distribution (KERD) studies, particularly for shedding more light on the elementary steps involved in the reductive H_2 elimination. From the detailed analysis of the experimental results, a mechanistic scheme for this reaction is deduced. Thus, based on these and earlier experimental studies the following sequence of elementary steps depicted in *Scheme 1* was proposed to rationalize the observed elimination reactions.

The initial step is insertion of the iron cation in a C–H or C–C bond. The resulting species, **I**, **II**, and **III**, can further rearrange *via* β-H or β-CH_3 shifts to form the intermediates **IV** and **V** which are the direct precursors for the elimination of H_2 or CH_4 [2b, c]. In addition to the sequential route for the H_2 loss ($Fe^+ + C_3H_8 \rightarrow$ **I**/**II** $\rightarrow$ **IV** $\rightarrow Fe(C_3H_6)^+ + H_2$), a second, concerted mechanism circumventing the dihydrido intermediate **IV** was postulated by *van Koppen et al.* [19] in order to explain the observation of the nonstatisti-

Scheme 1

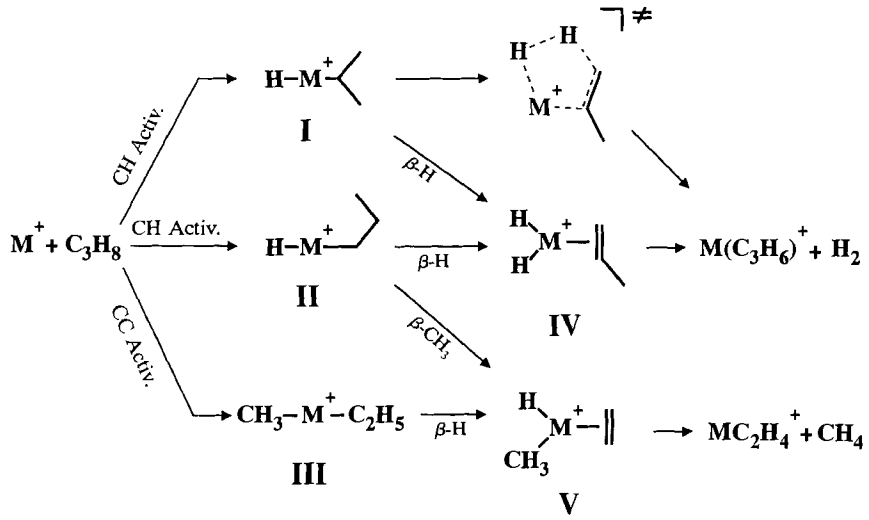

cal, bimodal KERDs for H_2 elimination. It should be noted at this point, that this latter interpretation is in agreement with our earlier quantum-chemical investigations on the C–H bond activation of ethane by Fe^+ and Co^+ [5], where no dihydrido minimum corresponding to **IV** could be located, in spite of being frequently postulated. Rather, a concerted mechanism was identified in these studies as the decisive step on the reaction coordinate. Following an interpretation by *Low* and *Goddard* as well as *Blomberg et al.* [20] of theoretical results for comparable reactions in *neutral* systems, *van Koppen et al.* assume that the activation barrier for the initial C–C insertion step is significantly higher than for the C–H insertion and lies above the energy of $Fe^+ + C_3H_8$. Therefore, the C–C bond activation path $Fe^+ + C_3H_8 \rightarrow$ **III** $\rightarrow$ **V** $\rightarrow Fe(C_2H_4)^+ + CH_4$ is explicitly excluded by these authors [19]. It is rather postulated that both reactions proceed through a joint intermediate **II** with the rate-determining step being the initial insertion of Fe^+ into the C–H bond. The activation barrier for this saddle point was given as 1.7 kcal mol^{-1} below the entrance channel, Fe (^{6}D) + C_3H_8. In this train of thought, the preference for CH_4 loss over H_2 elimination is due to a more demanding activation barrier for the latter process later on the reaction coordinate. From isotopic labeling studies, it was concluded that the barriers must be determined by transition states connected with the formation or cleavage of a C–H bond. In addition, *van Koppen et al.* provided various energetic details of the PES of $[FeC_3H_8]^+$, which will be discussed in the appropriate parts of the following exposition of our computational study.

C–C Bond Activation. – *Scheme 2* shows the computed C–C activation branch of the PES of $[FeC_3H_8]^+$, while the optimized structures of all relevant minima and saddle points (together with the major components of the transition vectors) are collected below.

Similar to $Fe^+ + C_2H_6$ [5a, b], the initial interaction of the iron cation in its ^{6}D-atomic ground state and propane has to occur on the sextet surface; however, since the ground state of the primary adduct ion, **1**, as well as the remainder of the PES have only three unpaired electrons, an intersystem crossing to the quartet surface has to take place *en*

Scheme 2

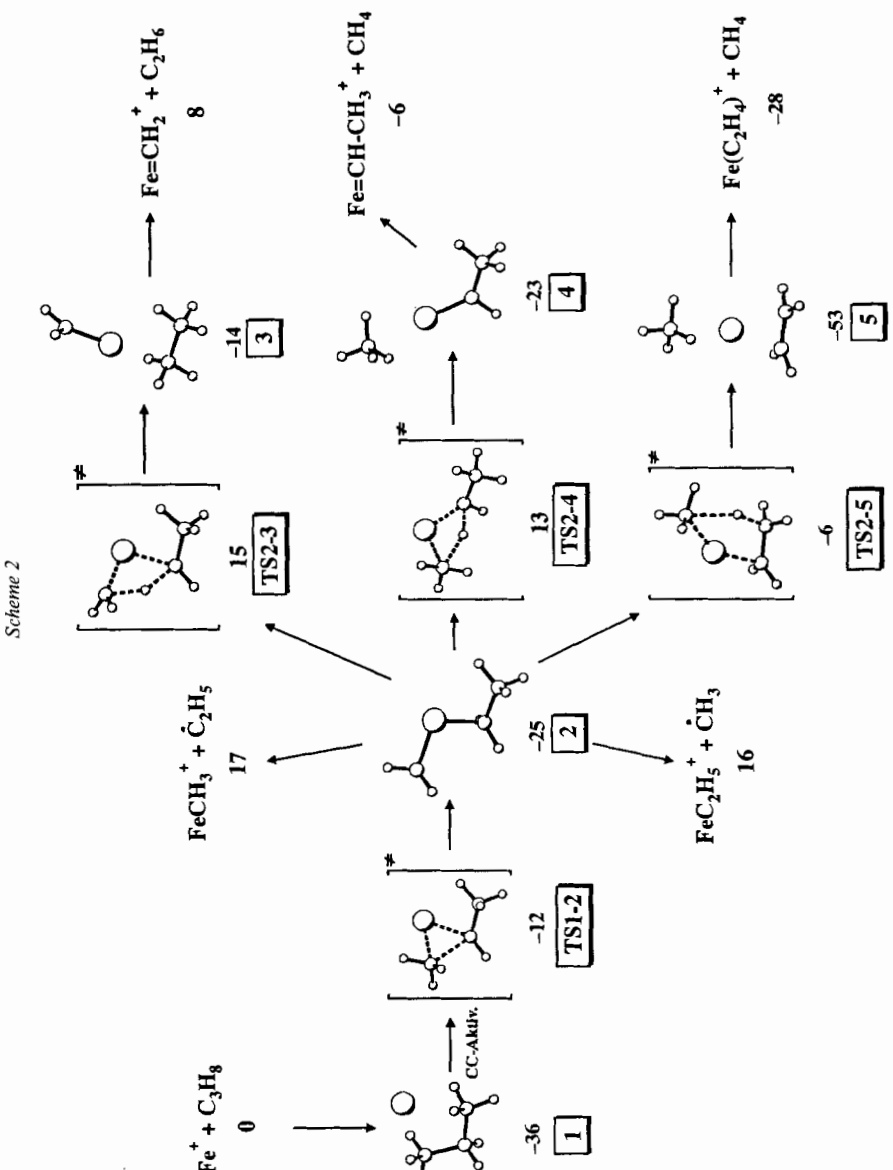
Fe+ + C3H8
0
CC-Aktiv.
–36
1
–12
TS1-2
–25
2
FeCH3+ + Ċ2H5
17
FeC2H5+ + ĊH3
16
15
TS2-3
–14
3
Fe=CH2+ + C2H6
8
13
TS2-4
–23
4
Fe=CH-CH3+ + CH4
–6
–6
TS2-5
–53
5
Fe(C2H4)+ + CH4
–28

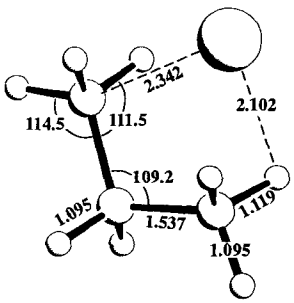
2.342
2.102
114.5
111.5
109.2
1.095
1.537
1.119
1.095

1

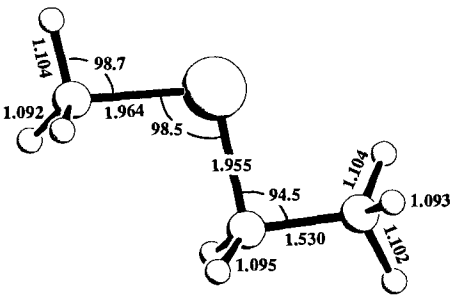
1.104
98.7
1.092
1.964
98.5
1.955
94.5
1.104
1.093
1.530
1.102
1.095

2

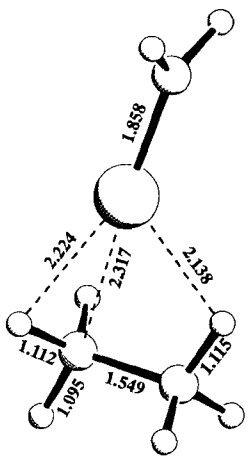
1.858
2.224
2.317
2.138
1.112
1.549
1.115
1.095

3

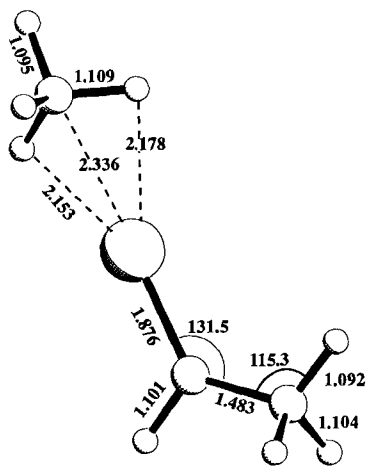
1.095
1.109
2.178
2.336
2.153
1.876
131.5
115.3
1.092
1.101
1.483
1.104

4

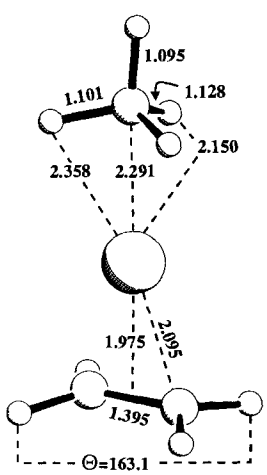
1.095
1.101
1.128
2.150
2.358
2.291
1.975
2.095
1.395
Θ=163.1

5

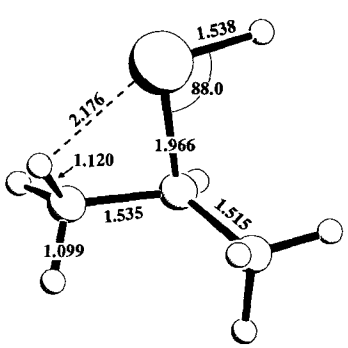
1.538
88.0
2.176
1.966
1.120
1.535
1.515
1.099

6

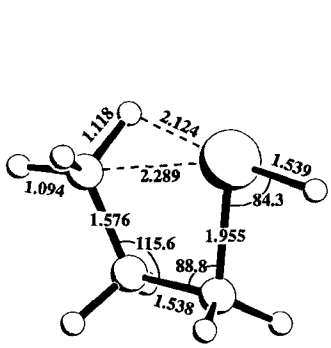

7

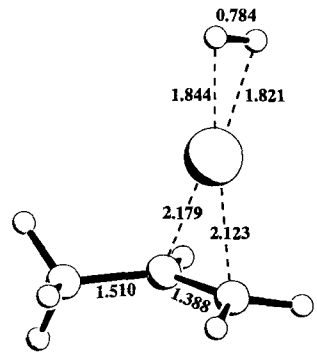

8

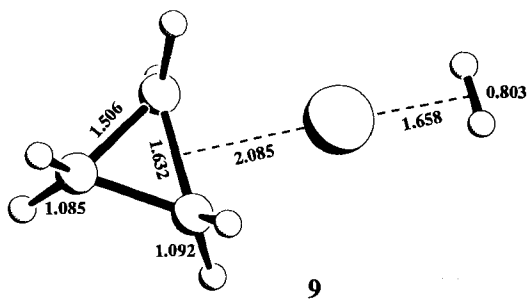

9

route from the separated reactants to the intermediate **1**. The same situation applies to the interactions of Fe^+ with ethane [5a, b]. In this case, typical vertical quartet-sextet excitation energies were between 20 and 40 kcal mol^{-1}, and thus, it is very unlikely that there will be a significant contribution of the sextet surface in the present context. While we did not explicitly compute the spin-orbit coupling matrix element, it is most probably large enough to allow for an efficient conversion to the energetically most favorable surface along the reaction coordinate, as discussed in detail for a related system by *Shaik et al.* [21]. It is a known phenomenon that transition-metal-mediated reactions very often occur on more than only one potential-energy surface [21]. The efficient switch from one surface to another brought about by spin-orbit coupling in such systems has in some instances been shown to have important consequences on the reaction mechanisms [21]. The interaction between Fe^+ and propane results in an encounter complex $Fe(C_3H_8)^+$. We localized three minimum isomers for this initial complex. The energetically most favored structure is the C_{2v}-symmetric species **1**. Here, the propane moiety keeps its staggered ground-state conformation. The Fe^+ has four identical contacts to H-atoms (*i.e.*, an η^4-coordination) with a Fe–H distance of 2.102 Å. Compared to separated propane, the C–H bond distances participating in the Fe^+–H interaction are elongated by 0.022 Å and the C–C–C angle decreased by 4°. The C–C distances are not affected by the presence of the Fe^+ ion. Species **1** is computed as 36 kcal mol^{-1} more stable than Fe^+ propane. The corresponding $Fe(C_2H_6)^+$ encounter complex was computed to lie 27 kcal mol^{-1} below the

separated species. The enhanced interaction energy in the propane system, which is also established experimentally (18 *vs.* 16 kcal mol^{-1}, resp.) is caused by the larger polarizability of the larger alkane, while its quantitative overestimation in our calculations is most likely a direct consequence of the problems of the current approach to describe the Fe^+ atomic-state separation mentioned above. In addition, our B3LYP/D95** calculations overestimate the increase in the average dipole polarizability when going from ethane to propane. While this increase experimentally amounts to 40% (ethane: 4.5 $Å^3$ *vs.* propane: 6.3 $Å^3$ [22]), we compute an increase of 47% (ethane: 3.4 $Å^3$ *vs.* propane: 5.0 $Å^3$). The other two isomers of this complex have C_s symmetry and the interaction of the iron cation with the H-atoms is η^3. These species are 4 and 8 kcal mol^{-1} less stable than **1** and are not considered further. **TS1-2** has been localized as saddle point for the insertion of the Fe^+ into a C–C bond. This transition structure is characterized by an imaginary frequency of 396*i* cm^{-1} and the transition vector corresponds to the expected components of the reaction coordinate, *i.e.*, breaking of one C–C bond with a concomitant rotation of the Me group. **TS1-2** is computed as 12 kcal mol^{-1} *below* the entrance channel. Thus, the initial C–C insertion step is connected with a rather low activation barrier and cannot represent the rate-limiting step along this reaction coordinate. While this result contradicts the hypothesis put forward by *van Koppen et al.* [19], it is consistent with the experimental observation in the Fe^+ + ethane system of a $Fe(C_2H_6)^+ \rightarrow H_3C{-}Fe^+{-}CH_3$ isomerization at thermal energies [23]. For this reaction, the activation barrier was computed as 7 kcal mol^{-1} below the $Fe^+ + C_2H_6$ asymptote [5b]. The even lower barrier in the present case is a consequence of the larger interaction energy of Fe^+ with the additional CH_2 group present in propane (*cf. Scheme 3*). **TS1-2** connects the initial complex with the C–C-inserted species **2**. This species adopts C_1 symmetry and is computed to be 11 kcal mol^{-1} less stable than **1** or 25 kcal mol^{-1} below the separated reactants. Starting from **2**, several options for proceeding on the PES are possible. In addition to two direct fragmentation processes $\mathbf{2} \rightarrow FeC_2H_5 + \dot{C}H_3$ and $\mathbf{2} \rightarrow FeCH_3^+ + \dot{C}_2H_5$ (41 and 42 kcal mol^{-1} above **2**, resp.), three different reaction paths, leading to the complexes **3**, **4**, and **5**, have been studied. The energetically most demanding among these three paths results in a C_s-symmetric complex between ethane and an iron-carbene cation, **3**, and occurs *via* saddle point **TS2-3** (imaginary frequency of 1453*i* cm^{-1}). Complex **3** is 14 kcal mol^{-1} below the entrance channel and 11 kcal mol^{-1} above **2**. Its equilibrium structure bears large similarity to the Fe^+-ethane and $H_2C{=}Fe^+{-}CH_4$ complexes found on the PES of $[FeC_2H_6]^+$ [5a, b]. Interestingly, the iron–carbene bond is not directed towards the midpoint of the ethane C–C bond but is tilted and points towards one of the C-atoms. However, for reaching **3** a sizable activation barrier of 40 kcal mol^{-1} (with respect to **2**) has to be surmounted. If compared to the energy of the entrance channel, the relative energy of **TS2-3** amounts to 15 kcal mol^{-1} above this asymptote. Thus, the direct fragmentation processes mentioned above are competitive with the generation of **3** *via* **TS2-3**. In concert with the experimental observations, no loss of ethane is expected even at elevated kinetic energies, due to the higher entropic demands of the compact transition structure **TS2-3** as compared to the direct bond cleavages. If, starting from **2**, a H-atom migrates from the central C-atom to one of the terminal ones (*i.e.*, in the opposite direction than discused above), species **4**, a complex between CH_4 and a cationic iron-ethylidene species, is formed. This complex is only 2 kcal mol^{-1} less stable than **2** (or 23 kcal mol^{-1} below the Fe^+ + propane asymptote), *i.e.*, energetically more favored than the related $H_2C{=}Fe^+{-}C_2H_6$ complex **3** by 9 kcal

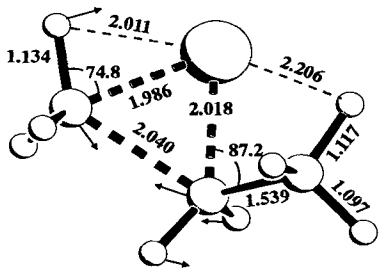

TS1-2

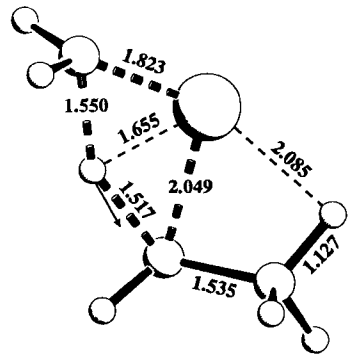

TS2-3

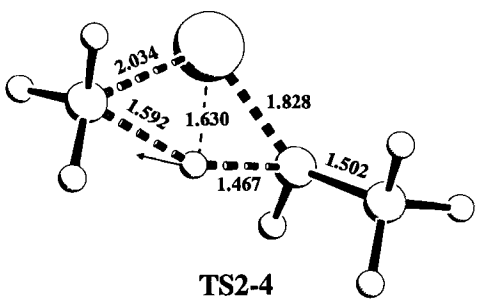

TS2-4

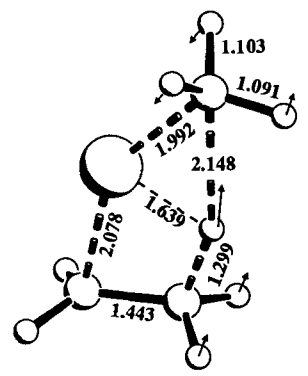

TS2-5

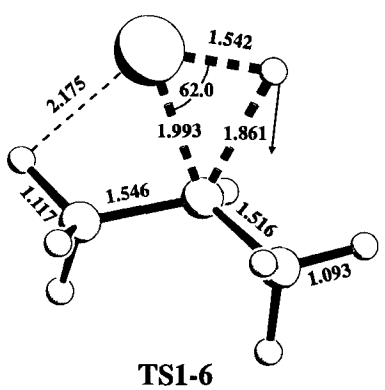

TS1-6

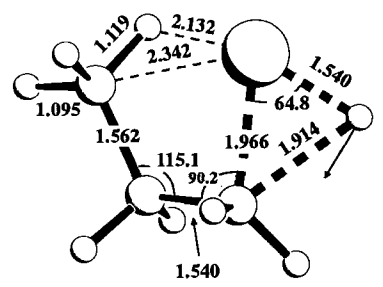

TS1-7

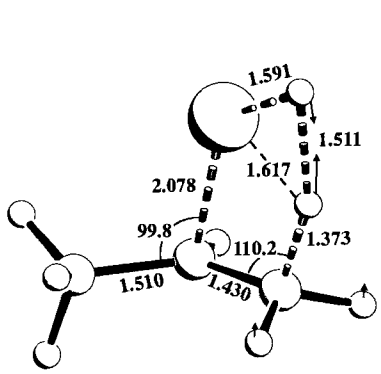

TS6-8

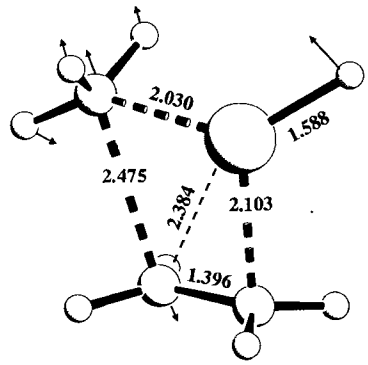

TS5-7

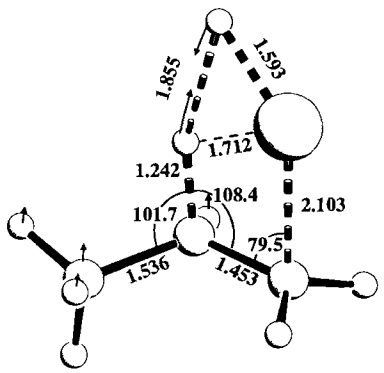

TS7-8

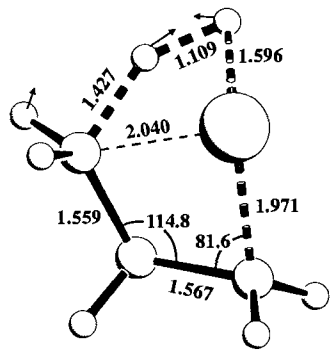

TS7-9

mol^{-1}. However, the saddle point connected with this H migration (**TS2-4**) exhibits a relative energy of 38 kcal mol^{-1} with respect to **2**, and is thus similarly demanding as **TS2-3**. Following the line of argumentation presented above for the absence of the elimination of ethane, it seems very unlikely that this process can effectively compete with the direct fragmentation processes. Consequently, the experimentally observed loss of CH_4 should not be due to the sequence **2** → **TS2-4** → **4** → $Fe{=}CH{=}CH_3^+ + CH_4$. In addition, the overall exothermicity of this process with respect to the $Fe^+ + C_3H_8$ asymptote of 6 kcal mol^{-1} is most likely only a consequence of the severe underestimation of the stability of the entrance channel (see above). Finally, the third reaction channel originating from **2** leads to **5**. This intermediate represents a cationic iron complex with CH_4 and ethylene. Complex **5** is significantly more stable than either **3** or **4** and is computed to be considerably below the entrance channel and the relative energy of **2** by 53 and 28 kcal mol^{-1}, respectively. The C_s-symmetric structure of **5** is characterized by a slightly distorted η^3-CH_4 entity bound to the Fe-atom (r(C–Fe) = 2.291 Å), which in turn is η^2-coordinated to the ethylene unit (r(C–Fe) = 2.095 Å). Its C–C bond distance is elongated as compared to the bond length in separated ethylene (Δr(C–C) = 0.054 Å) and the CH_2 groups are bent away from the metal. Complex **5** acts as a direct precursor for the elimination of CH_4, the computed exothermicity of the overall reaction,

$Fe^+ + C_3H_8 \rightarrow Fe(C_2H_4)^+ + CH_4$, amounts to 28 kcal mol^{-1}. The experimental value estimated by *van Koppen et al.* amounts to only 17 kcal mol^{-1} [19], reflecting problems of the B3LYP approach to satisfactorily describe the $Fe^+ + C_3H_8$ asymptote, as discussed in the section *Calibration*. On the other hand, *van Koppen et al.* also estimated the threshold for CH_4 extrusion from **5** (*i.e.*, for the process $\mathbf{5} \rightarrow Fe(C_2H_4)^+ + CH_4$) as 23.3 ± 1.0 kcal mol^{-1} and the relative stability of **5** with respect to **1** as 20 kcal mol^{-1} [17]. Both values are in good agreement with our corresponding theoretically predicted results of 25 and 17 kcal mol^{-1}, respectively, demonstrating the internal consistency of our calculations. The saddle point separating **2** from **5** (**TS2-5**) is characterized by an imaginary frequency of $403i\ cm^{-1}$, and the major components of the transition vector unambiguously indicate the migration of a β-H-atom onto the Me group and the concomitant reorientation of this Me group to give **5**. **TS2-5** is connected with an activation barrier with respect to **2** of 19 kcal mol^{-1} and lies even 6 kcal mol^{-1} below the $Fe^+ + C_3H_8$ asymptote. Thus, this reaction is only about half as demanding as the other two rearrangements originating from **2**. As a consequence, the exothermic elimination of CH_4 observed experimentally at thermal energies can occur *via* the sequence $\mathbf{2} \rightarrow \mathbf{TS2\text{-}5} \rightarrow Fe(C_2H_4)^+ + CH_4$. This pathway for the reductive elimination of CH_4 is in distinct contrast to the mechanistic scenario suggested by *van Koppen et al.* for this reaction. As already indicated in *Experimental Background*, these authors explicity ruled out that the loss of CH_4 occurs *via* a C–C-inserted species. Instead, they postulated a mechanism where the initial step is the insertion in a C–H bond. We will return to this hypothesis in the next section.

C–H Bond Activation. – We now turn to the C–H bond-activation part of the $[FeC_3H_8]^+$ PES. The geometrical details of the relevant stationary points are also collected above, while *Scheme 3* contains a sketch of the theoretically predicted energy profile.

Commencing from the encounter complex **1**, which is common to both the C–C and C–H bond-activation branches, two alternative routes for C–H bond activation are possible, depending on whether the Fe^+ initially inserts into a C–H bond from the terminal or the central C-atom. In the following, we will discuss both alternatives side by side. The saddle points for insertion into a central and terminal C–H bond are **TS1-6** ($526i\ cm^{-1}$) and **TS1-7** ($444i\ cm^{-1}$), respectively. In both cases, the activation barrier amounts to 21 kcal mol^{-1} with respect to **1**, which has to be compared with a barrier height of 24 kcal mol^{-1} for the insertion of Fe^+ into the C–C bond (**TS1-2**). The geometrical parameters as well as the major components of the transition vectors show the expected behavior. The corresponding C–H-inserted minima, *i.e.*, **6** and **7** are only marginally more stable than the transition structures, being 16 and 17 kcal mol^{-1} below the entrance channel. A very similar situation was already observed in the corresponding Fe^+- and Co^+-mediated C–H bond-activation processes in ethane [5]. Both, **6** and **7** can isomerize in a concerted (as opposed to a step-wise) fashion to the same product **8**, a cationic iron complex with H_2 and propene. This species is 36 kcal mol^{-1} below the entrance asymptote and represents the precursor for the exothermic elimination of H_2. The two saddle points relating **6** and **7** with **8**, *i.e.*, **TS6-8** and **TS7-8**, show imaginary frequencies of $1019i$ and $431i\ cm^{-1}$, respectively, and are located at 3 kcal mol^{-1} below and 2 kcal mol^{-1} above the energy of the separated reactants, Fe^+ + propane. In spite of a careful search, no indications for the existence of the previously postulated dihydrido species **IV** (see *Scheme 1*) were found. This is in complete accord with our earlier

Scheme 3

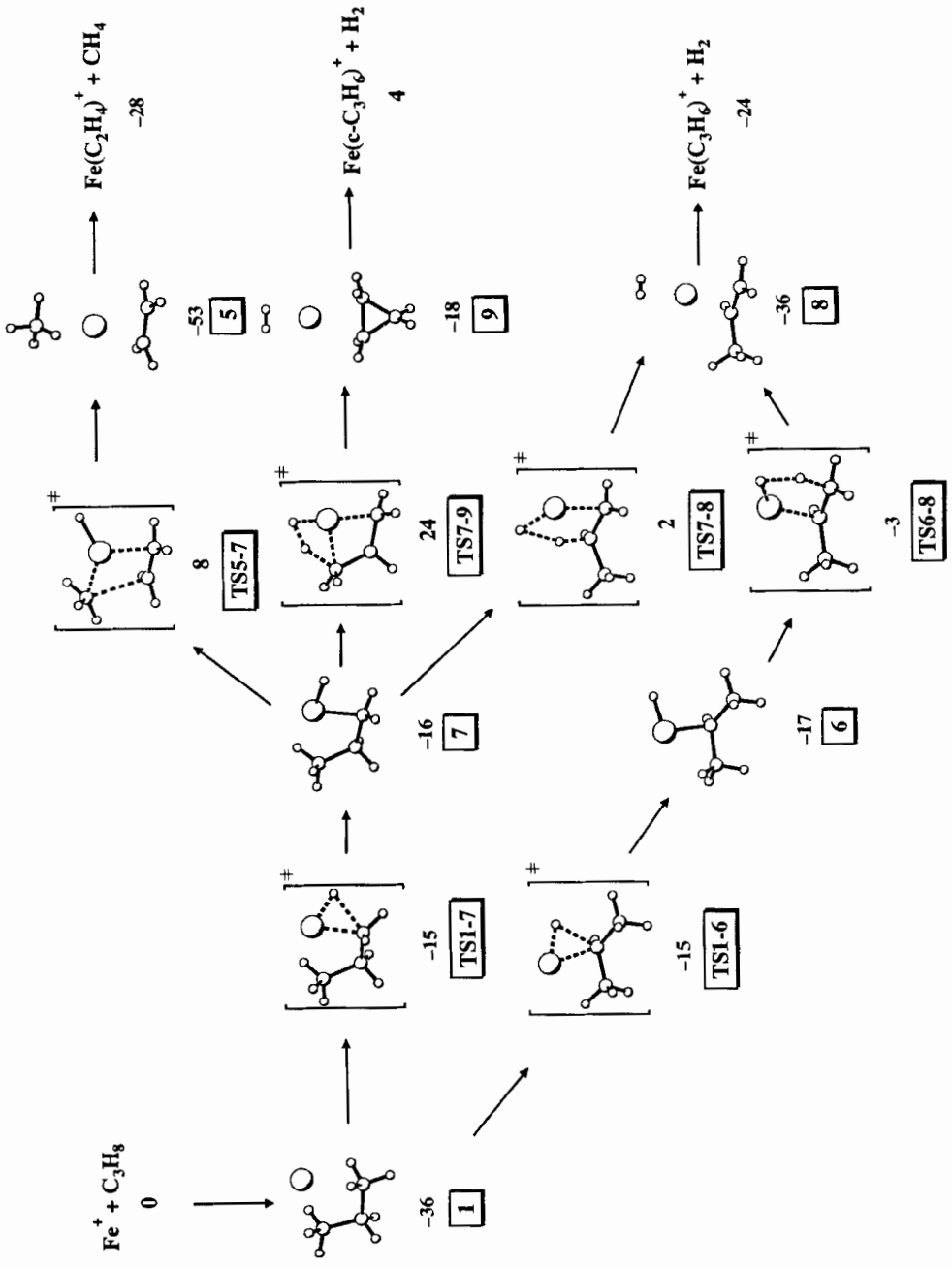
Fe+ + C3H8
0
1
–36
TS1-7
–15
7
–16
TS5-7
8
5
–53
Fe(C2H4)+ + CH4
–28
TS7-9
24
9
–18
Fe(c-C3H6)+ + H2
4
TS1-6
–15
6
–17
TS7-8
2
8
–36
Fe(C3H6)+ + H2
–24
TS6-8
–3

investigations on the C–H bond activations in ethane by Fe^+ and Co^+, where the existence of such species could also be excluded by calculations [5][5]). Rather, in these as well as in the present case, the rate-determining steps for the reductive elimination of H_2 are concerted rearrangements directly connecting the C–H-inserted species with the precursor complex for H_2 loss. It is tempting to relate the existence of two, energetically similar pathways for reaching **8** with the experimental observation of two different reaction mechanisms for the H_2 elimination [19]. However, a detailed theoretical analysis of the underlying KERD experiments would require to include dynamical aspects of these reactions, which is beyond the scope of the present work.

Stepping back to the C–H-inserted species **7**, two additional reaction sequences were studied. As already mentioned above, at the heart of the postulated mechanistic picture of *van Koppen et al.* for the reductive CH_4 elimination is their assumption that this process occurs as a sideway from the C–H-inserted species [19]: this mechanism starts with the insertion of the Fe^+ cation into a primary C–H bond of propane. This species would then undergo a β-H shift generating an intermediate **V** (*Scheme 1*) which acts as the precursor for the expulsion of CH_4. However, all our attempts to localize a hydrido-methyl species **V** on the PES of $[FeC_3H_8]^+$ were unsuccessful and led directly to either **5** or **7**[6]). The only species which, in terms of its geometry, bears some similarity to **V** is **TS5-7** representing the saddle point (imaginary frequency of $309i$ cm^{-1}) for the conversion of **7** into **5** as proved by calculation of the intrinsic reaction coordinate[7]). Thus, an alternative route for the CH_4 elimination appears to be the sequence **7** → **TS7-7** → **5** → $Fe(C_2H_4)^+$, akin to the mechanism proposed by *van Koppen et al.* However, the relative energy of the decisive transition structure in this sequence (**TS5-7**) amounts to 24 and 8 kcal mol^{-1} with respect to **7** and the entrance channel. Hence, our calculations indicate that the reductive elimination of CH_4 *does not occur via* the mechanism suggested by *van Koppen et al.* Rather, the energetically significantly more favored pathway as described in the previous section commences with the C–C-inserted species **2** and leads through the rate-determining saddle point **TS2-5** to **5** and subsequently to the products. The energy difference between **TS2-5** and **TS5-7**, which exhibit similar binding situations, amounts to 12 kcal mol^{-1} and is thus large enough to exclude that this preference is merely due to an artifact of the computational strategy. As already alluded to above, the lines of argument employed by *van Koppen et al.* to exclude a mechanism involving a C–C-inserted species for the reductive elimination of CH_4 are mainly influenced by the conclusions drawn by *Low* and *Goddard* [20a–c] from their investigations of the barrier heights of the insertion of Pt and Pd into H–H, C–H, and C–C bonds in *neutral* systems. Although M–H and M–C single bonds have similar bond energies, they found that the barriers increased in

---

[5]) In fact, dihydrido minima do exist for earlier first-row transition-metal ions in the gas phase. For $HScH^+$, see [24].

[6]) It is interesting to note that no Fe^+-dihydrido- or hydrido-methyl species exist, while the corresponding methyl-ethyl cation (**2**) as well as the dimethyl species [5a, b] do represent stable minima. This can probably be related to the differences in binding energies: A C–C bond is weaker than a C–H bond (*ca.* 90 *vs.* 105 kcal mol^{-1}), but at the same time a Fe^+–H bond is weaker than a Fe^+–C bond (*ca.* 49 *vs.* 55 kcal mol^{-1}). In addition, the alkyl groups attached to an iron cation exert a stabilizing agostic interaction, not possible for a H-atom. Based on these arguments dihydrido minima should be the least stable ones, followed by H–Fe^+–R and finally R–Fe^+–R′ as the most stable species.

[7]) For details of the IRC approach, see [25].

the order H–H, C–H, and C–C, because of the more pronounced directionality of a C(sp^3)–M bond as compared to a bond involving a spherical H-atom. Thus, the hydrogen 1s orbital can interact simultaneously with the metal and the alkyl group, while breaking the C–C bond and forming the C–M bond requires a reorientation of the Me group which leads to an increase of the activation barriers. Similar results were also obtained in the recent extensive work of *Siegbahn* and coworkers [20d, e]. However, in the present case we are dealing with *positively charged* species, where in addition to these effects, further issues have to be considered. *E.g.*, **TS1-2** profits from two stabilizing agostic interactions between the cationic iron center and hydrogens from the two Me groups, as indicated by the rather short H–Fe contacts of 2.011 and 2.206 Å. On the other hand, only one such interaction is visible in **TS1-6** and **TS1-7** (r(Fe–H) = 2.175 and 2.132 Å, resp.). It should also be noted, that *van Koppen et al.* rationalize the experimentally observed preference of CH_4 elimination over loss of H_2 by postulating a *lower* activation barrier for the making of the C–H bond from intermediate **V** (*Scheme 1*) as compared to the formation of the H–H bond from species **IV** [19]. But this interpretation now clearly contradicts the *Low-Goddard* model [20]: the more pronounced directionality of the Me group should lead to a *higher* and not a lower barrier for the C–H as compared to the H–H bond formation.

Finally, we studied the possibility of a [1,3]-H_2 elimination from **7** as a potential alternative to the [1,2] eliminations *via* **TS6-8** and **TS7-8**. [1,3] Eliminations of H_2 are experimentally known to occur in the Sc^+ + propane and Ti^+ + propane systems [26]. However, even though a reaction channel for such an elimination could be located, leading *via* **TS7-9** to the complex **9** as precursor for the expulsion of H_2, it cannot compete with the [1,2] eliminations: **TS7-9** is located 24 kcal mol^{-1} above the Fe^+ + propane asymptote, over 20 kcal mol^{-1} more demanding than the transition structures connected with the [1,2] eliminations. In agreement with this finding, no indications of an [1,3]-H_2 loss were observed in the isotopic labeling experiments by *van Koppen et al.* [19].

In conclusion, while the present quantum-chemical investigation leads to mechanistic scenarios for the C–H and C–C bond activations in propane brought about by a bare Fe^+ cation that differ substantially from those previously suggested by *van Koppen et al.*, our results are nevertheless consistent with all experimental information. The experimentally deduced relative energy of the rate-determining step for the C–H bond activation of −1.7 kcal mol^{-1} below the entrance channel is in good accord with the theoretically predicted relative stability of **TS6-8** of −3 kcal mol^{-1}. Also, the preference of CH_4 loss over H_2 loss finds its straightforward explanation in the fact that the decisive saddle point for the former process (**TS2-5**) is 3 kcal mol^{-1} more favorable than the highest point on the C–H bond-activation reaction coordinate (**TS6-8**). Finally, the theoretically predicted course of the C–H bond-activation in propane bears large similarities, both in terms of the energetical demands of the saddle points and the geometrical details of the transition structures, to the mechanism proposed earlier for the transition-metal-ion mediated H_2 loss from ethane [5].

Conclusions. – The structural and energetical details of the PES pertinent to the Fe^+-mediated C–C and C–H bond-activation processes in propane have been investigated computationally employing the B3LYP density-functional theory/*Hartree-Fock*

hybrid method in combination with adequately flexible one-particle basis sets. The following conclusions emerge from this study:

i) Our calculations provide an internally consistent picture of the C–H and C–C bond-activation processes and are in agreement with all available experimental facts.

ii) The processes observed experimentally at thermal energies, *i.e.*, elimination of CH_4 and H_2, are also computationally characterized by low activation barriers and to proceed entirely below the energy of the entrance channel, $Fe^+ + C_3H_8$. All other possible processes require activation energies significantly above the energy of the separated reactants.

iii) The initial insertions of Fe^+ into a C–H or C–C bond are energetically much less demanding than the subsequent rearrangement reactions, which lead to the precursor complexes for the reductive elimination of CH_4 and H_2. In agreement with the earlier findings for the interaction between Fe^+ + ethane and Co^+ + ethane, these rate-determining rearrangements are concerted in nature.

iv) The calculations do not support the earlier mechanistic proposal for the course of the C–C bond-activation process. Instead of proceeding from a C–H bond-inserted intermediate, the present study identifies a reaction path originating from the C–C-inserted species as the energetically most favored one.

v) The decisive transition structure for the loss of CH_4 is predicted as 3 kcal mol^{-1} less demanding than the energetic bottleneck for the H_2 elimination, in complete accord with the experimentally determined ratio of 3:1 for these two processes.

vi) The absence of any indication for a [1,3] elimination of H_2 in the isotopic labelling experiments is corroborated by the calculations, in which a much higher activation barrier for this mechanism as opposed to [1,2] eliminations is predicted.

vii) For those stationary points on the PES of $[FeC_3H_8]^+$, which have a counterpart on the PES of $[FeC_2H_6]^+$, very similar geometries and even relative energies are obtained.

This last observations is of particular interest in light of our anticipated studies on the Fe^+-mediated C–C and C–H bond-activation processes in larger alkanes. It opens the possibility to employ the transition structures computed in the present investigation as building blocks for generating the corresponding saddle-point geometries in the more complex systems. Thus, the extremely demanding full geometry optimizations in such large systems, which are prohibitive with the computational resources available to us, are circumvented. Studies along these lines showing very promising results are close to completion and will be published soon [27].

This work was supported by the *Deutsche Forschungsgemeinschaft*, the *Fonds der Chemischen Industrie* and the *Gesellschaft von Freunden der Technischen Universität Berlin*. A significant amount of computer time and excellent services (Dr. *T. Steinke*) were provided by the *Konrad Zuse* Zentrum für Informationstechnik, Berlin, and by the Zentraleinrichtung Rechenzentrum at TU Berlin. Helpful discussions with Dr. *D. Schröder* are gratefully acknowledged. *M.C.H.* thanks Prof. *H. Schwarz* for financial support. Finally, we thank the referee for helpful comments.

REFERENCES

[1] J. Haggin, *Chem. Eng. News* **1993**, *71*, 27.

[2] a) D. Schröder, H. Schwarz, *Angew. Chem.* **1995**, *107*, 2126; *ibid. Int. Ed.* **1995**, *34*, 1973; b) B. S. Freiser, *Acc. Chem. Res.* **1994**, *27*, 353; c) K. Eller, H. Schwarz, *Chem. Rev.* **1991**, *91*, 1121; d) P. B. Armentrout, in 'Selective Hydrocarbon Activation', Eds, J. A. Davis, P. L. Watson, J. F. Liebmann, and A. Greenberg, VCH, New York, 1990.

[3] C.W. Bauschlicher, Jr., S.R. Langhoff, H. Partridge, in 'Modern Electronic Structure Theory, Part II', Ed. D.R. Yarkony, World Scientific, Singapore, 1995.

[4] a) M.C. Holthausen, C. Heinemann, H.H. Cornehl, W. Koch, H. Schwarz, *J. Chem. Phys.* **1995,** *102,* 4931; b) M.C. Holthausen, M. Mohr, W. Koch, *Chem. Phys. Lett.* **1995,** *240,* 245; c) C. Heinemann, H. Schwarz, W. Koch, K.G. Dyall, *J. Chem. Phys.* **1996,** *104,* 4642; d) A. Ricca, C.W. Bauschlicher, Jr., *Chem. Phys. Lett.* **1995,** *245,* 150; e) A. Ricca, C.W. Bauschlicher, Jr., *Theor. Chim. Acta* **1995,** *92,* 123; f) A. Ricca, C.W. Bauschlicher, Jr., *J. Phys. Chem.* **1995,** *99,* 5922; g) V. Barone, *Chem. Phys. Lett.* **1995,** *233,* 129; V. Barone, *J. Phys. Chem.* **1995,** *99,* 11659; i) C. Adamo, F. Lelj, *Chem. Phys. Lett.* **1995,** *246,* 463; j) V. Barone, C. Adamo, *J. Phys. Chem.* **1996,** *100,* 2094.

[5] a) M.C. Holthausen, A. Fiedler, H. Schwarz, W. Koch, *Angew. Chem.* **1995,** *107,* 2430; *ibid. Int. Ed.* **1995,** *34,* 2282; b) M.C. Holthausen, A. Fiedler, H. Schwarz, W. Koch, *J. Phys. Chem.* **1996,** *100,* 6236; c) M.C. Holthausen, W. Koch, *J. Am. Chem. Soc.,* in press.

[6] a) A.D. Becke, *J. Chem. Phys.* **1993,** *98,* 5648; *ibid.* **1993,** *98,* 1372; b) P.J. Stephens, F.J. Devlin, C.F. Chabalowski, M.J. Frisch, *J. Phys. Chem.* **1994,** *98,* 11623.

[7] Gaussian 92/DFT, Rev. F.2: M.J. Frisch, G.W. Trucks, H.W. Schlegel, P.M.W. Gill, B.G. Johnson, M.W. Wong, J.B. Foresman, M.A. Robb, M. Head-Gordon, E.S. Replogle, R. Gomperts, J.L. Andres, K. Raghavachari, J.S. Binkley, C. Gonzales, R.L. Martin, D.J. Fox, D.J. DeFrees, J. Baker, J.J.P. Stewart, J.A. Pople, Gaussian, Inc., Pittsburg, PA, 1992.

[8] T.H. Dunning, P.J. Hay, in 'Modern Theoretical Chemistry, Vol. II', Ed. H.F. Schaefer, III, Plenum Press, New York, 1977.

[9] A.J.H. Wachters, *J. Chem. Phys.* **1970,** *52,* 103.

[10] P.J. Hay, *J. Chem. Phys.* **1977,** *66,* 4377.

[11] a) B.G. Johnson, M.J. Frisch, *Chem. Phys. Lett.* **1993,** *216,* 133; b) B.G. Johnson, P.M.W. Gill, J.A. Pople, *ibid.* **1994,** *220,* 377.

[12] B.L. Kickel, P.B. Armentrout, in 'Organometallic Ion Chemistry', Ed. B.S. Freiser, Kluwer, Dordrecht, 1996.

[13] C.E. Moore 'Atomic Energy Levels', Natl. Bureau of Standards (USA), Circ. 467: Washington, DC, 1949.

[14] a) O. Gunnarson, R.O. Jones, *Phys. Rev. B: Condens. Matter* **1985,** *31,* 7588; b) T. Ziegler, J. Li *Can. J. Chem.* **1994,** *72,* 783.

[15] R. van Leeuwen, E.J. Baerends, *Int. J. Quantum Chem.* **1994,** *52,* 711.

[16] S.G. Lias, J.E. Bartmess, J.F. Liebman, J.L. Holmes, R.D. Levin, W.G. Mallard, *J. Phys. Ref. Data, Suppl.* **1988,** *17,* 1.

[17] D. Schröder, H. Schwarz, *J. Organomet. Chem.* **1995,** *504,* 123.

[18] a) P.A.M. van Koppen, P.R. Kemper, M.T. Bowers, *J. Am. Chem. Soc.* **1992,** *114,* 10941; b) R.H. Schultz, P.B. Armentrout, *ibid.* **1991,** *113,* 729; c) R.H. Schultz, J.L. Elkind, P.B. Armentrout, *ibid.* **1988,** *110,* 411; d) R.H. Schultz, P.B. Armentrout, *J. Phys. Chem.* **1987,** *91,* 4433; e) D.B. Jacobson, B.S. Freiser, *J. Am. Chem. Soc.* **1983,** *105,* 5197; f) R. Houriet, L.F. Halle, J.L. Beauchamp, *Organometallics* **1983,** *2,* 1818; g) L.F. Halle, P.B. Armentrout, J.L. Beauchamp, *ibid.* **1982,** *1,* 963; h) G.D. Byrd, R.C. Burnier, B.S. Freiser, *J. Am. Chem. Soc.* **1982,** *104,* 3565.

[19] P.A.M. van Koppen, M.T. Bowers, E.R. Fisher, P.B. Armentrout, *J. Am. Chem. Soc.* **1944,** *116,* 3780.

[20] a) J.J. Low, W.A. Goddard, III, *J. Am. Chem. Soc.* **1984,** *106,* 8321; b) *ibid.* **1986,** *108,* 6115; c) *Organometallics* **1986,** *5,* 609; d) M.R.A. Blomberg, P.E.M. Siegbahn, U. Nagashima, J. Wennerberg, *J. Am. Chem. Soc.* **1991,** *113,* 424; e) M.R.A. Blomberg, U. Brandemark, P.E.M. Siegbahn, *ibid.* **1983,** *105,* 5557.

[21] a) S. Shaik, D. Danovich, A. Fiedler, D. Schröder, H. Schwarz, *Helv. Chim. Acta,* **1995,** *78,* 1393; b) A. Fiedler, D. Schröder, S. Shaik, H. Schwarz, *J. Am. Chem. Soc.* **1994,** *116,* 10734; c) H.H. Cornehl, C. Heinemann, D. Schröder, H. Schwarz, *Organometallics* **1995,** *14,* 992.

[22] A.A. Radzig, B.F. Smirnov, 'Atomic and Molecular Reference Data', Springer Verlag, Heidelberg–Berlin, 1986.

[23] R.H. Schultz, P.B. Armentrout, *J. Chem. Phys.* **1992,** *96,* 1662.

[24] J.E. Bushnell, P.R. Kemper, P. Maitre, M.T. Bowers, *J. Am. Chem. Soc.* **1994,** *116,* 9710.

[25] a) C. Gonzales, H.B. Schlegel, *J. Chem. Phys.* **1989,** *90,* 2154; b) K. Fukui, *J. Phys. Chem.* **1970,** *74,* 4161.

[26] a) L.S. Sunderlin, P.B. Armentrout, *Organometallics* **1990,** *9,* 1248; b) M.A. Tolbert, J.L. Beauchamp, *J. Am. Chem. Soc.* **1984,** *106,* 8117.

[27] a) M.C. Holthausen, G. Hornung, D. Schröder, H. Schwarz, W. Koch, in preparation; b) M.C. Holthausen, Ph.D. thesis, TU Berlin, 1996.